



Joint Reference Microphone Selection and Filter Order Determination in Multi-channel Active Noise Control

De Hu*, Shuyao Liu, Yanrong He

College of Computer Science, Inner Mongolia University, China

cshood@imu.edu.cn, syliu@mail.imu.edu.cn, yrhe@mail.imu.edu.cn

Abstract

Multi-channel active noise control (MCANC) systems have been widely investigated for acoustic noise attenuation over a spatial region. In MCANC systems, incorporating more reference microphones (RMs) can boost noise reduction performance but increase the computational complexity, which may affect real-time processing capability. To improve the computational efficiency, we propose a joint approach for RM selection and filter order (FO) determination in MCANC systems. The optimal RM subset is selected by promoting group sparsity in filter coefficients while constraining the output noise power. The optimal FO is determined by encouraging the consecutive highest-order filter coefficients to approach zero under the specified performance constraint. By combining the above two criteria, we formulate a novel cost function that enables simultaneous RM selection and FO determination. In addition, we present a re-weighting strategy to further reduce both the number of selected RMs and the FO value. Numerical simulations confirm the validity of the proposed method.

Index Terms: Multi-channel active noise control, reference microphone selection, filter order determination, group sparsity

1. Introduction

Active noise control (ANC) [1–3] plays an important role in various audio signal processing scenarios, including headrests [4], headphones [5], and automotive fields [6, 7], to name but a few. The traditional single-channel feedforward ANC system typically uses a reference microphone (RM) to capture the noise signal as input for the ANC controller. Then the “antinoise” is generated and played through the loudspeaker to cancel the noise at the control point. To cope with more complex noise environments, such as those with multiple or moving noise sources, multi-channel ANC (MCANC) systems have emerged as the need arises. One property of MCANC systems is that the more RMs adopted, the better the noise reduction performance. However, with increasing RMs, the computational load increases significantly, which may result in poor real-time capability.

To improve computational efficiency, recent advances are moving toward implementing MCANC after selecting an informative RM subset. Specifically, Hase *et al.* [8] proposed an RM selection method based on causality constraints (CC), which first estimates the time difference of arrival (TDoA) between each RM and the error microphone (EM) and then selects the RM that satisfies causality. Recently, the study [9] analyzed the impact of the coherence between RM signals and EM signals, which concludes that the RM with a higher coherence coefficient makes a greater contribution to the MCANC procedure. Based on [9], Shen *et al.* [10] developed a coherence-

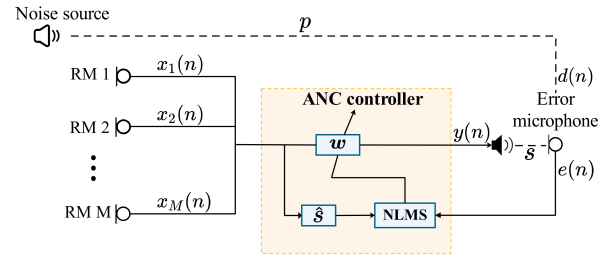


Figure 1: Block diagram of the MCANC system.

based RM selection method based on the rank of coherence coefficients. Subsequently, a coherence-based weight determination scheme [11] was presented for multi-channel wireless active noise control headphone systems, which can be seen as a more general case of [10]. Nevertheless, both causality-based and coherence-based criteria do not directly reflect the noise reduction effect, thus it is questionable whether using them is beneficial in MCANC systems.

Another key factor affecting the system’s computational complexity is the filter order (FO) of adaptive filters. Generally, a higher FO improves noise reduction performance but increases the computational complexity. Moreover, adaptive filters tend to converge more slowly with a larger FO. Therefore, how to determine the optimal FO of adaptive filters is very important. However, to the best of our knowledge, most existing approaches determine the FO empirically rather than seeking an optimal one based on specific scenarios.

In this work, we propose a joint method for RM selection and FO determination to optimize computational efficiency in MCANC systems. To be specific, we first develop an RM selection approach by formulating a novel cost function, which induces the group sparsity of filter coefficients while constraining the output noise power. Then, by introducing an auxiliary vector, we construct another cost function to determine the optimal FO, where the consecutive highest-order filter coefficients are encouraged to approach zero. Afterward, we establish the final cost function by combining the above two cost functions, from which the optimal RM subset and FO can be determined simultaneously. Finally, we adopt a re-weighting strategy to further reduce both the number of selected RMs and the value of FO. Numerical experimental results demonstrate the efficacy of the proposed method in terms of computational efficiency.

2. Fundamentals

As shown in Fig. 1, the considered MCANC system consists of M spatially distributed RMs, a loudspeaker (act as the sec-

*Corresponding Author.

ondary source), and an EM (at the control position). RMs capture and transmit the reference signals to the ANC controller, which carries out the multiple channel filtered-x normalized least mean square (MCFxNLMS) algorithm [12–14], followed by playing the “antinoise” through the loudspeaker to cancel the noise at the control point. Let n be the time index, the control signal $y(n)$, i.e., the “antinoise”, can be generated as

$$y(n) = \sum_{m=1}^M \mathbf{w}_m^T(n) \mathbf{x}_m(n), \quad (1)$$

where \mathbf{w}_m is the control filter of the m -th RM and \mathbf{x}_m is the vector that contains the signal received by the m -th RM, i.e.,

$$\mathbf{w}_m(n) = [w_{m,1}(n), w_{m,2}(n), \dots, w_{m,J}(n)]^T, \quad (2)$$

$$\mathbf{x}_m(n) = [x_m(n), x_m(n-1), \dots, x_m(n-J+1)]^T, \quad (3)$$

where J is the FO, and $(\cdot)^T$ represents the transpose operation. Based on above, the error signal $e(n)$ is given by

$$e(n) = d(n) - \mathbf{y}^T(n) \mathbf{s}(n), \quad (4)$$

where $\mathbf{y}(n) = [y(n), y(n-1), \dots, y(n-K+1)]^T$, $d(n)$ is the unwanted noise through the primary path $\mathbf{p}(n)$, also referred to as the desired signal, and $\mathbf{s}(n)$ is the secondary path with a length of K .

The optimal filter coefficients can be deduced by minimizing the mean square error (MSE) $\mathbb{E}\{e^2(n)\}$ with $\mathbb{E}\{\cdot\}$ denoting the mathematical expectation. However, $\mathbb{E}\{e^2(n)\}$ requires all samples in $e(n)$, which is not suitable for real-time processing. Instead, the MCFxNLMS algorithm minimizes the instantaneous error signal $e(n)$ by using the following recursive formula

$$\mathbf{w}_m(n+1) = \mathbf{w}_m(n) + \frac{\eta}{\beta + \sum_{m=1}^M \|\mathbf{x}'_m(n)\|_2^2} \mathbf{x}'_m(n) e(n), \quad (5)$$

where $\|\cdot\|_2$ represents the ℓ_2 -norm, η is the step-size, β is the regularization parameter, and $\mathbf{x}'_m(n) = [x'_m(n), x'_m(n-1), \dots, x'_m(n-J+1)]^T$ with $x'_m(n) = \mathbf{r}_m^T(n) \hat{\mathbf{s}}(n)$ in which $\mathbf{r}_m(n) = [x_m(n), x_m(n-1), \dots, x_m(n-K+1)]^T$ and $\hat{\mathbf{s}}(n)$ is the estimate of $\mathbf{s}(n)$. In practice, $\hat{\mathbf{s}}(n)$ can be obtained before the ANC procedure [15, 16]. Furthermore, $d(n)$ is not directly accessible and needs to be estimated from the error signal, i.e., $\hat{d}(n) = e(n) + \mathbf{y}^T(n) \hat{\mathbf{s}}(n)$. For the MCFxNLMS algorithm, theoretically, more RMs lead to better noise reduction performance. However, as the number M of RMs increases, the computational load and transmission power increase significantly. To overcome this deficiency, recent advances in MCANC systems are moving toward using informative RMs to conduct the MCFxNLMS algorithm [8, 10].

3. Proposed Method

To improve computational efficiency, we propose a joint method of RM selection and FO determination. Similarly to the study [8, 10], here we consider using N samples to carry out the method. In this case, the error signal in (4) can be reformulated in a vector form as

$$\mathbf{e} = \mathbf{A} \mathbf{w} - \hat{\mathbf{d}}, \quad (6)$$

with

$$\mathbf{e} = [e(1), e(2), \dots, e(N)]^T, \quad (7a)$$

$$\hat{\mathbf{d}} = [\hat{d}(1), \hat{d}(2), \dots, \hat{d}(N)]^T, \quad (7b)$$

$$\mathbf{w} = [\mathbf{w}_1^T, \mathbf{w}_2^T, \dots, \mathbf{w}_M^T]^T, \quad (7c)$$

$$\mathbf{A} = [\mathbf{X}'_1 \mathbf{X}'_2 \dots \mathbf{X}'_M], \quad (7d)$$

where $\mathbf{X}'_m = [\mathbf{x}'_m(1), \mathbf{x}'_m(2), \dots, \mathbf{x}'_m(N)]$. Note that \mathbf{w}_m is the time-invariant version of $\mathbf{w}_m(n)$, which represents the optimal filter of RM m during RM selection and FO determination.

3.1. RM selection using group sparsity

When minimizing (6) with respect to \mathbf{w} , if the solution for \mathbf{w}_m contains all zeros, it can be inferred that the received signal from RM m is unused, and therefore RM m can be switched to sleep mode. To promote such group sparsity [17] in \mathbf{w} , we formulate the following optimization problem, which minimizes the $\ell_{0,2}$ -norm of \mathbf{w} while constraining the output noise power (i.e. error signal power) with a pre-specified parameter P_0 , i.e.,

$$\begin{aligned} \min_{\mathbf{w}} \quad & \|\mathbf{w}\|_{0,2} \\ \text{subject to} \quad & (C1): \frac{1}{N} \|\mathbf{A} \mathbf{w} - \hat{\mathbf{d}}\|_2^2 \leq P_0, \end{aligned} \quad (8)$$

where $\|\mathbf{w}\|_{0,2}$ indicates the $\ell_{0,2}$ -norm of \mathbf{w} , which is defined by

$$\|\mathbf{w}\|_{0,2} = \|[\|\mathbf{w}_1\|_2, \|\mathbf{w}_2\|_2, \dots, \|\mathbf{w}_M\|_2]\|_0, \quad (9)$$

where $\|\cdot\|_0$ denotes the ℓ_0 -norm. In practice, however, it is challenging to solve (8) due to the non-convexity of the ℓ_0 -norm. Here, inspired by the literature [18, 19], we relax the $\ell_{0,2}$ -norm into the following $\ell_{1,2}$ -norm

$$\|\mathbf{w}\|_{1,2} = \|[\|\mathbf{w}_1\|_2, \|\mathbf{w}_2\|_2, \dots, \|\mathbf{w}_M\|_2]\|_1 = \sum_{m=1}^M \|\mathbf{w}_m\|_2, \quad (10)$$

with $\|\cdot\|_1$ being the ℓ_1 -norm. By substituting the $\ell_{0,2}$ -norm in (8) with the $\ell_{1,2}$ -norm, another optimization problem can be constructed as

$$\begin{aligned} \min_{\mathbf{t}, \mathbf{w}} \quad & \mathbf{1}_M^T \mathbf{t} \\ \text{subject to} \quad & (C1), \\ & (C2): \|\mathbf{w}_m\|_2 \leq t_m, \quad m = 1, 2, \dots, M, \end{aligned} \quad (11)$$

where $\mathbf{t} = [t_1, t_2, \dots, t_M]^T$ is the introduced selection vector, and $\mathbf{1}_M$ is the M dimensional all-one vector. The problem (11) is convex and thus can be solved efficiently. If the solution \hat{t}_m of t_m is zero, it indicates that the m -th RM is unselected.

Remark I: The pre-specified parameter P_0 can be calculated as $P_0 = P/\alpha_0$, where P is the error signal power obtained by activating all RMs for MCANC and $\alpha_0 \in (0, 1)$ is an adjustable parameter.

3.2. FO determination

As we mentioned earlier, FO is another factor that affects computational efficiency. Given an empirically defined filter order J , we present an FO determination method in this subsection.

3.2.1. The auxiliary vector construction

When minimizing (6) with respect to \mathbf{w} , if Q consecutive highest-index elements in the solution of \mathbf{w}_m are equal to zero, we can determine the order of \mathbf{w}_m as $J - Q$. In other words, to determine the appropriate FO, we should make as many consecutive highest-index filter coefficients as possible approach zeros. To this end, we introduce an auxiliary vector $\tilde{\mathbf{t}}$ as

$$\tilde{\mathbf{t}} = \begin{bmatrix} \tilde{t}_1 \\ \tilde{t}_2 \\ \vdots \\ \tilde{t}_J \end{bmatrix} = \begin{bmatrix} \bar{w}_1 + \bar{w}_2 + \dots + \bar{w}_J \\ \bar{w}_2 + \dots + \bar{w}_J \\ \vdots \\ \bar{w}_J \end{bmatrix}, \quad (12)$$

where $\bar{w}_j = \sum_{m=1}^M |w_{m,j}|$ with $w_{m,j}$ being the j -th element of \mathbf{w}_m . Obviously, $\bar{w}_j = \tilde{t}_j - \tilde{t}_{j+1}$ for $j < J$ and $\bar{w}_j = \tilde{t}_j$ for $j = J$. Taking the ℓ_0 -norm of $\tilde{\mathbf{t}}$ and applying the triangle inequality [20], we have

$$\begin{aligned} \|\tilde{\mathbf{t}}\|_0 &= \sum_{j=1}^J \left\| \sum_{i=j}^J \bar{w}_i \right\|_0 \leq \sum_{j=1}^J \sum_{i=j}^J \|\bar{w}_i\|_0 \\ &= \sum_{j=1}^J j \|\bar{w}_j\|_0. \end{aligned} \quad (13)$$

According to (13), the filter coefficients with higher indices are assigned higher weights. Therefore, when minimizing $\|\tilde{\mathbf{t}}\|_0$, the filter coefficients with higher indices are preferentially penalized to zero. In doing so, we can determine the FO by removing those consecutive zero-valued elements with the highest indices.

3.2.2. FO determination

By substituting the ℓ_0 -norm in (13) with ℓ_1 -norm and applying performance constraint (C1), we can obtain the following FO determination problem

$$\begin{aligned} \min_{\tilde{\mathbf{t}}, \mathbf{w}} \quad & \mathbf{1}_J^T \tilde{\mathbf{t}} \\ \text{subject to} \quad & (C1), \\ & (C3) : \bar{w}_j \leq \tilde{t}_j - \tilde{t}_{j+1}, \\ & j = 1, 2, \dots, J, \end{aligned} \quad (14)$$

where $\tilde{t}_{m,J+1} = 0$ is a constant. As the feasibility domain of $\bar{w}_j = \tilde{t}_j - \tilde{t}_{j+1}$ is a non-convex set, we relax it to an inequality in (C3). As a result, problem (14) also involves convex programming, which can be solved efficiently.

3.3. Joint RM selection and FO determination

To simultaneously carry out RM selection and FO determination, we can combine problems (11) and (14) as follows

$$\begin{aligned} \min_{\tilde{\mathbf{t}}, \tilde{\mathbf{t}}} \quad & (1 - \lambda) \mathbf{1}_M^T \mathbf{t} + \lambda \mathbf{1}_J^T \tilde{\mathbf{t}} \\ \text{subject to} \quad & (C1), (C2), (C3). \end{aligned} \quad (15)$$

where $0 \leq \lambda \leq 1$ represents the trade-off parameter. Due to the fact that both (11) and (14) are convex, the overall problem (15) is also convex and can be solved using existing solvers like CVX [21] or SeDuMi [22].

3.4. Sparsity promoting via re-weighting strategy

To further improve computational efficiency, we adopt a re-weighting strategy to induce sparsity both in \mathbf{t} and $\tilde{\mathbf{t}}$. Specifically, we replace $\mathbf{1}_M$ and $\mathbf{1}_J$ in (15) with $\mathbf{u}^{(l)}$ and $\tilde{\mathbf{u}}^{(l)}$, respectively, obtaining

$$\begin{aligned} \min_{\tilde{\mathbf{t}}, \tilde{\mathbf{t}}} \quad & (1 - \lambda) \mathbf{t}^T \mathbf{u}^{(l)} + \lambda \tilde{\mathbf{t}}^T \tilde{\mathbf{u}}^{(l)} \\ \text{subject to} \quad & (C1), (C2), (C3), \end{aligned} \quad (16)$$

where $\mathbf{u}^{(l)} = [u_1^{(l)}, u_2^{(l)}, \dots, u_M^{(l)}]^T$ and $\tilde{\mathbf{u}}^{(l)} = [\tilde{u}_1^{(l)}, \tilde{u}_2^{(l)}, \dots, \tilde{u}_J^{(l)}]^T$ are assigned weights in the l -th re-weighting iteration. Inspired by [23, 24], we can update $\mathbf{u}^{(l)}$

and $\tilde{\mathbf{u}}^{(l)}$ via the following criterion

$$u_m^{(l+1)} = \frac{1}{t_m^{(l)} + \varepsilon_1}, \quad (17a)$$

$$\tilde{u}_m^{(l+1)} = \frac{1}{\tilde{t}_m^{(l)} + \varepsilon_2}, \quad (17b)$$

where ε_1 and ε_2 are small constants that can prevent the denominator from being zero. According to (17a) and (17b), a larger $t_m^{(l)}$ or $\tilde{t}_m^{(l)}$ in the l -th iteration will result in a smaller $u_m^{(l+1)}$ or $\tilde{u}_m^{(l+1)}$ in the next iteration, which enables the small elements in $t_m^{(l)}$ or $\tilde{t}_m^{(l)}$ to be penalized aggressively, hence encouraging them to be zero with the iteration progressing. Since both \mathbf{t} and $\tilde{\mathbf{t}}$ can be represented by \mathbf{w} , the above iteration procedure can be terminated when the change in \mathbf{w} becomes smaller than a small threshold θ .

Finally, we can run the MCFxNLMS algorithm using the selected RM subset with the determined FO. We would like to note that we should set $\text{FO} = J$ and activate all RMs to execute the MCFxNLMS algorithm before the proposed method is complete.

4. Simulation Results

The simulation environment is an enclosure of size $3 \text{ m} \times 3 \text{ m}$, where 2 noise sources, 20 RMs, 1 secondary source, and 1 EM are randomly distributed (Fig. 2). The noise sources play two real recorded noises from the dataset [25]. Besides, the sampling rate is set to 16 kHz; the signal length N for RM selection and FO determination is set to 48000 samples (which is equivalent to 3 seconds); the step size η in (5) and the initial FO J are fixed to $\eta = 1 \times 10^{-3}$ and $J = 50$, respectively; the secondary path length K and the threshold θ below (17) are fixed to $K = 27$ and $\theta = 1 \times 10^{-2}$, respectively; the parameters β in (5), ε_1 and ε_2 in (17) are empirically set to 1×10^{-6} .

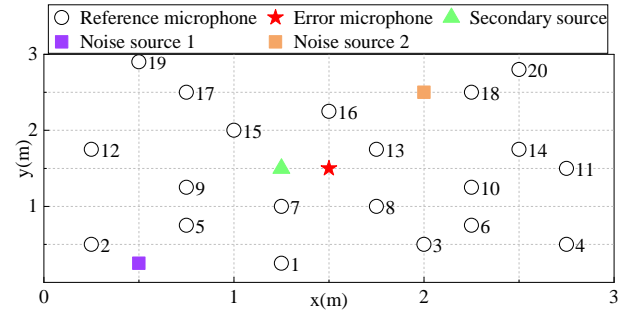


Figure 2: Geometry configuration, including 2 noise sources, 20 RMs, 1 secondary source, and 1 EM in an enclosure.

In the subsequent experiments, we use the noise reduction ratio (NRR) as the evaluation metric, which is defined by

$$\text{NRR} = 10 \log_{10} \frac{\sum_{n=1}^{N_{LMS}} e^2(n)}{\sum_{n=1}^{N_{LMS}} d^2(n)}, \quad (18)$$

where N_{LMS} represents the signal length during MCFxLMS filtering, which is set to $N_{LMS} = 160000$ samples. In other words, we adopt the first 3 seconds of the signals for RM selection and FO determination and then employ the last 10 seconds of the signals to evaluate the noise reduction performance using the MCFxLMS algorithm.

4.1. RM selection and FO determination results during re-weighting iterations

To validate the effectiveness of the re-weighting strategy, in this simulation, we evaluate RM selection and FO determination in each re-weighting iteration when $\alpha_0 = 0.9$ and $\lambda = 0.5$. Fig. 3 shows the results in the first 3 re-weighting iterations, since the re-weighting strategy converges in 3 iterations. In Fig. 3(a), $t_m = 0$ indicates that the m -th RM is unselected, thus the number of selected RMs decreases from 9 to 3 when l increases from 1 to 3. In Fig. 3(b), the largest non-zero FO index can be seen as the obtained FO, thus the FO decreases from 40 to 34 when l increases from 1 to 3. Based on the above phenomenon, we can conclude that the re-weighting strategy can further improve computational efficiency under the specified performance constraint (C1), due to the fact that the performance constraint (C1) can always be ensured when solving (15).

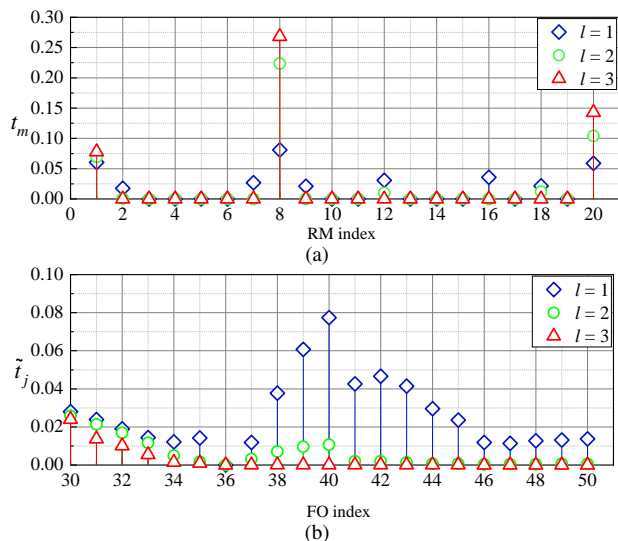


Figure 3: RM selection and FO determination during re-weighting iteration process: (a) RM selection results; (b) FO determination results.

4.2. Effectiveness of joint RM selection and FO determination

In order to demonstrate the necessity of joint RM selection and FO determination method, we test the performance of MCANC when $\lambda = \{0.0, 0.5, 1.0\}$: if $\lambda = 0.0$, the optimization problem (15) degrades into an RM selection problem; if $\lambda = 1.0$, the optimization problem (15) degrades into an FO determination problem; if $\lambda = 0.5$, the optimization problem (15) becomes a joint problem of RM selection and FO determination. We set $\alpha_0 = \{0.5, 0.7, 0.9\}$ to display the results under different noise reduction constraints. In addition to NRR, we compute the number of multiply-accumulate operations [26], i.e.,

$$\text{Complexity} = 2MJ + MK + 1,$$

to evaluate the computational complexity of the MCANC system. As shown in Fig. 4, the NRRs of all methods are comparable for the same α_0 , while the computational complexity of the joint method ($\lambda = 0.5$) is always lower than that of the RM selection method ($\lambda = 0.0$) and the FO determination method ($\lambda = 1.0$). This experiment illustrates the superiority of the proposed method in terms of computational efficiency.

4.3. Comparison experiment

In this simulation, we test the noise reduction effect under different performance constraints by setting different values of α_0 .

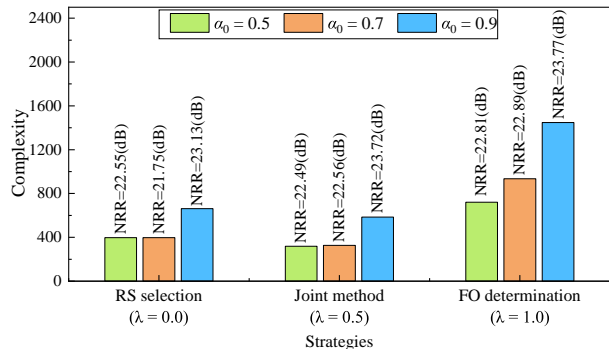


Figure 4: Complexity of RM selection, FO determination, and joint RM selection and FO determination.

Comparison approaches include the CC approach [8] and the coherence-based selection (CBS) approach [11]. For the sake of fairness, we keep the size of the selected RM subset of the CC and CBS approaches consistent with that of the proposed method. To be specific, we randomly select M_0 RMs from the RM subset that satisfy the causality constraints in the CC approach and choose M_0 RMs with the largest coherence coefficients in the CBS approach, where M_0 is the size of the RM subset in the proposed method. As shown in Table 1, the proposed method always provides the highest NRR and possesses the lowest complexity, thus outperforming the CC and CBS approaches in terms of computational efficiency. Note that the FO of the CC and CBS approaches is consistently equal to $J = 50$, as they do not involve FO determination. Based on the complexity formula $2M_0J + M_0K + 1$, the complexity of the CC and CBS approaches is identical under the same number of selected RMs.

Table 1: Comparison of noise reduction performance with varying numbers of RMs

	α_0	0.3	0.5	0.7	0.9	0.95
The num. M_0 of RMs		2	3	3	4	5
FO	Proposed	38	38	42	43	45
	CC [8]	50	50	50	50	50
	CBS [11]	50	50	50	50	50
NRR(dB)	Proposed	20.2027	22.4956	22.5621	23.7269	24.2644
	CC [8]	19.2291	20.5202	20.5202	20.6141	22.7983
	CBS [11]	18.3952	20.7156	20.8306	21.8006	21.3864
Complexity	Proposed	207	310	334	453	586
	CC [8]	255	382	382	509	636
	CBS [11]	255	382	382	509	636

5. Conclusions

This paper proposed a joint method for RM selection and FO determination in MCANC systems. Specifically, after constraining the output noise power with a predefined threshold, the RMs were selected by inducing the group sparsity in filter coefficients, while the FO was determined by pushing the consecutive highest-order filter coefficients to zeros. Additionally, a re-weighting strategy was presented to further reduce the RM number and the FO value. The experimental results demonstrated that the proposed method outperforms existing RM selection methods in terms of computational efficiency. In our future work, we will study how to jointly optimize the RM subset, the FO, and the loudspeaker subset in a more general MCANC system with multiple RMs and multiple secondary sources.

6. Acknowledgements

This work was supported by the National Natural Science Foundation of China under Grants 62201297 and 62361045.

7. References

- [1] S. M. Kuo and D. R. Morgan, "Active noise control: a tutorial review," *Proceedings of the IEEE*, vol. 87, no. 6, pp. 943–973, Jun. 1999.
- [2] Y. Kajikawa, W. S. Gan, and S. M. Kuo, "Recent advances on active noise control: open issues and innovative applications," *AP-SIPA Transactions on Signal and Information Processing*, vol. 1, no. 1, p. e3, Aug. 2012.
- [3] S. J. Elliott and P. A. Nelson, "Active noise control," *IEEE signal processing magazine*, vol. 10, no. 4, pp. 12–35, Oct. 1993.
- [4] S. Bagha, D. P. Das, and S. K. Behera, "Reference microphone free active headrest system for noise containing varying frequency tonal components," *IEEE Transactions on Circuits and Systems II: Express Briefs*, vol. 70, no. 8, pp. 3184–3188, Aug. 2023.
- [5] Y. Iotov, S. M. Nørholm, P. J. McCutcheon, and M. G. Christensen, "Improving speech attenuation in headphones using harmonic model decomposition and multiple-frequency ANC," in *IEEE International Conference on Acoustics, Speech and Signal Processing*, Seoul, Korea, 2024, pp. 1376–1380.
- [6] M. Zhang, Y. Zhang, and J. Chen, "Active noise cancellation in automotive applications," in *IEEE International Conference on Control Applications*, Dubrovnik, Croatia, 2017, pp. 1–4.
- [7] P. Ahamed and P. Duraiswamy, "Virtual sensing active noise control system with 2D microphone array for automotive applications," in *International Conference on Signal Processing and Integrated Networks*, Noida, India, 2019, pp. 151–155.
- [8] S. Hase, Y. Kajikawa, L. Liu, and S. M. Kuo, "Multi-channel ANC system using optimized reference microphones based on time difference of arrival," in *European Signal Processing Conference*, Nice, France, 2015, pp. 305–309.
- [9] J. A. Zhang, N. Murata, Y. Maeno, P. N. Samarasinghe, and T. D. Abhayapala, "Coherence-based performance analysis on noise reduction in multichannel active noise control systems," *The Journal of the Acoustical Society of America*, vol. 148, no. 3, pp. 1519–1528, Sep. 2020.
- [10] X. Shen, D. Shi, and W. S. Gan, "A wireless reference active noise control headphone using coherence based selection technique," in *IEEE International Conference on Acoustics, Speech and Signal Processing*, Ontario, Canada, 2021, pp. 7983–7987.
- [11] X. Shen, D. Shi, S. Peksi, and W. S. Gan, "A multi-channel wireless active noise control headphone with coherence-based weight determination algorithm," *Journal of Signal Processing Systems*, vol. 94, no. 8, pp. 811–819, Mar. 2022.
- [12] S. Mohapatra and A. Kar, "A review on filtered-x LMS algorithm," in *International Conference on Electrical Engineering/Electronics, Computer, Telecommunications and Information Technology*, Hua Hin, Thailand, 2015, pp. 1–5.
- [13] M. T. Akhtar and W. Mitsuhashi, "A modified normalized FxLMS algorithm for active control of impulsive noise," in *European Signal Processing Conference*, Aalborg, Denmark, 2010, pp. 1–5.
- [14] M. Chen, Y. Guo, Z. Geng, and L. Li, "Filtered-x least mean square/power normalized fourth algorithm (FXLMS/PF) for active noise control," in *IEEE International Conference on Mechatronics and Automation*, Heilongjiang, China, 2023, pp. 1322–1327.
- [15] H. Hassanpour and P. Davari, "An efficient online secondary path estimation for feedback active noise control systems," *Digital Signal Processing*, vol. 19, no. 2, pp. 241–249, Mar. 2009.
- [16] M. Hu and J. Lu, "Active control of line spectral noise with simultaneous secondary path modeling without auxiliary noise," in *IEEE International Conference on Acoustics, Speech and Signal Processing*, Barcelona, Spain, 2020, pp. 466–470.
- [17] A. Lohmann, T. van Waterschoot, J. Bitzer, and S. Doclo, "Microphone subset selection for the weighted prediction error algorithm using a group sparsity penalty," in *IEEE International Conference on Acoustics, Speech and Signal Processing*, Seoul, Korea, 2024, pp. 1101–1105.
- [18] M. B. Hawes and W. Liu, "Sparse microphone array design for wideband beamforming," in *International Conference on Digital Signal Processing*, Santorini, Greece, 2013, pp. 1–5.
- [19] D. Wipf and S. Nagarajan, "Iterative reweighted ℓ_1 and ℓ_2 methods for finding sparse solutions," *IEEE Journal of Selected Topics in Signal Processing*, vol. 4, no. 2, pp. 317–329, Feb. 2010.
- [20] A. Jiang, H. K. Kwan, Y. Zhu, X. Liu, N. Xu, and Y. Tang, "Design of sparse FIR filters with joint optimization of sparsity and filter order," *IEEE Transactions on Circuits and Systems I: Regular Papers*, vol. 62, no. 1, pp. 195–204, Jan. 2015.
- [21] M. Grant and S. Boyd, "CVX: Matlab software for disciplined convex programming, version 2.1," Sep. 2013. [Online]. Available: <http://cvxr.com/cvx>
- [22] J. F. Sturm, "Using SeDuMi 1.02, a MATLAB toolbox for optimization over symmetric cones," *Optimization methods and software*, vol. 11, no. 2, pp. 1–4, Aug. 1999.
- [23] R. Chartrand and Y. Wotao, "Iteratively reweighted algorithms for compressive sensing," in *IEEE International Conference on Acoustics, Speech and Signal Processing*, NV, USA, 2008, pp. 3869–3872.
- [24] L. Shuang, "Sparse representation of hardy function by iteratively reweighted least squares," in *International Symposium on Computer Engineering and Intelligent Communications*, Guangzhou, China, 2020, pp. 57–60.
- [25] C. K. Reddy, E. Beyrami, J. Pool, R. Cutler, S. Srinivasan, and J. Gehrke, "A scalable noisy speech dataset and online subjective test framework," in *Interspeech*, Graz, Austria, 2019, pp. 1816–1820.
- [26] C. Shi and Y. Kajikawa, "A partial-update minimax algorithm for practical implementation of multi-channel feedforward active noise control," in *International Workshop on Acoustic Signal Enhancement*, Tokyo, Japan, 2018, pp. 1–15.